HHS Public Access

Author manuscript

Sci Transl Med. Author manuscript; available in PMC 2018 January 04.

Published in final edited form as:

Sci Transl Med. 2012 February 22; 4(122): 122ra22. doi:10.1126/scitranslmed.3003441.

MicroRNA-21 Blocks Abdominal Aortic Aneurysm Development and Nicotine-Augmented Expansion

Lars Maegdefessel[1], **Junya Azuma**[1], **Ryuji Toh**[1], **Alicia Deng**[1], **Denis R. Merk**[2], **Azad Raiesdana**[1], **Nicholas J. Leeper**[3], **Uwe Raaz**[1], **Anke M. Schoelmerich**[1], **Michael V. McConnell**[1], **Ronald L. Dalman**[3], **Joshua M. Spin**[1], and **Philip S. Tsao**[1,*]

[1]Division of Cardiovascular Medicine, Stanford University School of Medicine, Stanford, CA 94305, USA

[2]Department of Cardiothoracic Surgery, Stanford University School of Medicine, Stanford, CA 94305, USA

[3]Division of Vascular Surgery, Stanford University School of Medicine, Stanford, CA 94305, USA

Abstract

Identification and treatment of abdominal aortic aneurysm (AAA) remains among the most prominent challenges in vascular medicine. MicroRNAs are crucial regulators of cardiovascular pathology and represent possible targets for the inhibition of AAA expansion. We identified microRNA-21 (miR-21) as a key modulator of proliferation and apoptosis of vascular wall smooth muscle cells during development of AAA in two established murine models. In both models (AAA induced by porcine pancreatic elastase or infusion of angiotensin II), miR-21 expression increased

*To whom correspondence should be addressed. ptsao@stanford.edu.

SUPPLEMENTARY MATERIALS

www.sciencetranslationalmedicine.org/cgi/content/full/4/122/122ra22/DC1

Materials and Methods

Fig. S1. Ultrasound images; *Pten* in the non-aneurysmal area of the aorta, nicotine, and miR-21–modulating effects in hAECs.

Fig. S2. IL-6 and angiotensin II regulate miR-21 induction through NF-κB; AAD and *Pten* in nicotine and anti-21/pre-21–transduced mice; miR-21 expression in miR-21–modulated mice with PPE-induced AAA.

Fig. S3. Effects of miR-21 modulation in angiotensin II–induced AAA; *Mmp2* expression in elastase-infused ± nicotine supplementation in mice with PPE-induced AAA.

Fig. S4. Coexpression and regulation of PTEN and Mac-1 or smooth muscle α-actin; ancillary off-target effects of miR-21 modulation.

Fig. S5. Role of fibrosis in miR-21–modulated mice with PPE-induced AAA; expression of miRs targeting PTEN in hASMCs being up-regulated by nicotine.

Fig. S6. Proposed mechanism of miR-21 induction and modulation in AAA disease.

Table S1. Serum cotinine concentration measurements.

Table S2. Blood pressure measurements in nicotine- versus placebo-treated mice.

Table S3. Absolute measurements of the AAD in PPE-induced AAA.

Table S4. Absolute measurements of the AAD in miR-21–modulated mice with PPE-induced AAA.

Table S5. Absolute measurements of the AAD in angiotensin II–induced AAA.

Table S6. Absolute measurements of the AAD in miR-21–modulated mice with angiotensin II–induced AAA.

References

Author contributions: L.M. designed the research; performed mouse studies, transductions, cell culture studies, transfection experiments, and tissue staining; interpreted the data; and wrote the manuscript. J.A., R.T., A.D., D.R.M., A.R., N.J.L., and U.R. performed mouse studies and cell culture experiments, interpreted the data, and assisted with manuscript preparation. A.M.S. performed RNA extraction and sample acquisition and analyzed and interpreted the data. M.V.M. and R.L.D. performed data analysis and assisted with manuscript preparation. J.M.S. and P.S.T. designed the research, interpreted the data, and wrote the manuscript.

Competing interests: L.M., J.M.S., and P.S.T. have applied for a patent relating to miR-21 and protection from AAA development. The other authors declare that they have no competing interests.

as AAA developed. Lentiviral overexpression of miR-21 induced cell proliferation and decreased apoptosis in the aortic wall, with protective effects on aneurysm expansion. miR-21 overexpression substantially decreased expression of the phosphatase and tensin homolog (PTEN) protein, leading to increased phosphorylation and activation of AKT, a component of a pro-proliferative and antiapoptotic pathway. Systemic injection of a locked nucleic acid–modified antagomir targeting miR-21 diminished the pro-proliferative impact of down-regulated PTEN, leading to a marked increase in the size of AAA. Similar results were seen in mice with AAA augmented by nicotine and in human aortic tissue samples from patients undergoing surgical repair of AAA (with more pronounced effects observed in smokers). Modulation of miR-21 expression shows potential as a new therapeutic option to limit AAA expansion and vascular disease progression.

INTRODUCTION

Abdominal aortic aneurysm (AAA) is a significant cause of morbidity and mortality worldwide. Data from clinical studies encompassing different populations suggest that the prevalence is 2.4 to 16.9% in men and 0.5 to 2.2% in women over the age of 65 (1). The most feared clinical consequence of AAA progression is acute rupture, which carries a mortality of 80%. Sixty percent of patients with AAAs die of other cardiovascular causes, such as myocardial infarction or stroke, suggesting a relationship between AAAs and atherosclerosis (2).

Predictors of AAA growth include diameter of the aorta at diagnosis and active smoking (3). Some studies have demonstrated that the incidence and progression of AAA are also related to hypertension and age (4). However, smoking is considered to be the major modifiable risk factor for development of AAA. Indeed, AAA is more closely associated with cigarette smoking than any other tobacco-related disease except lung cancer. Most AAA patients (>90%) have a history of smoking (5).

MicroRNAs (miRNAs) are ~20-nucleotide, single-stranded RNA molecules that target mRNA through partial complementarity, thereby inhibiting translation or inducing mRNA degradation (6). Their role in AAA disease, as well as their therapeutic potential to inhibit aneurysm expansion, remains unknown.

MicroRNA-21 (miR-21) is one of the most commonly and markedly up-regulated miRNAs in several cardiovascular diseases, as well as in many cancers (7). miR-21 has several validated targets including phosphatase and tensin homolog (PTEN) (8, 9), sprouty-1 (SPRY1) (10), programmed cell death 4 (PDCD4) (11), and B cell lymphoma 2 (BCL2) (8), which could potentially link it to aneurysm pathology.

PTEN, a lipid and protein phosphatase and important tumor suppressor protein, acts as a key negative regulator of the phosphoinositide 3-kinase (PI3K) pathway by dephosphorylating membrane phosphatidylinositol 3,4,5-trisphosphate (12). PTEN is essential for regulation of both basal and growth factor–stimulated PI3K-mediated signaling. An increase in cellular phosphatidylinositol 3,4,5-trisphosphate in response to dysregulated PTEN activity, even in the absence of stimuli, is sufficient to activate numerous downstream effectors, most notably

AKT, extracellular signal–regulated kinase (ERK), and mammalian target of rapamycin (mTOR) (9, 13). In response to PI3K activation, the serinethreonine kinase AKT regulates the activity of a number of targets, including kinases, transcription factors, and other regulatory molecules, affecting a broad range of cellular functions such as proliferation, differentiation, migration, and cell survival (12). A growing body of information suggests that regulation of PTEN signaling plays a crucial role in vascular integrity and that alteration in PTEN signaling serves as a key initiating determinant driving pathological vascular remodeling.

Here, we investigated whether the regulatory effects of miR-21 and its putative gene targets that affect proliferation, apoptosis, and inflammation might offer a new therapeutic approach to limiting AAA disease.

RESULTS

Nicotine accelerates AAA expansion in mice

Given emerging evidence of the significant effects of the major tobacco component nicotine on vascular disease (14), we chose to investigate whether nicotine supplementation would accelerate AAA progression using the porcine pancreatic elastase (PPE) infusion model of AAA in 10-week-old male C57BL/6J mice. Nicotine (5 mg/60 days) or placebo pellets were implanted subcutaneously on the lateral shoulder 7 days before AAA induction (by PPE infusion). Cotinine (a breakdown product of nicotine) concentrations in nicotine-treated animal serum at four different time points after pellet implantation were comparable to those found in the serum of intermediate to heavy human smokers (table S1) (15). In elastase-infused mice, blood pressure measurements of nicotine-treated versus placebo-treated animals showed no differences at 14 days after pellet implantation (table S2). Brightness modulation (B-mode) ultrasound imaging performed 3, 7, 14, 21, and 28 days after PPE infusion showed a significant increase in expansion of the abdominal aortic diameter (AAD) from day 7 until day 28 for nicotine-supplemented mice compared with placebo-supplemented mice, and for both elastase-infused groups when compared with control mice receiving saline instead of elastase (“sham”; Fig. 1A; fig. S1A; table S3).

Up-regulation of miR-21 in AAA is enhanced by nicotine

Aortic miR-21 expression in the aneurysmal abdominal segment was markedly up-regulated in animals with elastase-induced AAAs compared with the equivalent segment in control animals. AorticmiR-21 expression was measured by TaqMan quantitative real-time polymerase chain reaction (qRT-PCR) at three different stages of AAA development and progression (7, 14, and 28 days after infusion of elastase) (Fig. 1B). In nicotine-supplemented animals, miR-21 expression was enhanced further at all three time points compared to placebo-supplemented as well as sham mice at days 14 and 28 (Fig. 1B). In situ hybridization (ISH) in AAA samples from the mice treated with elastase and nicotine or elastase alone confirmed that miR-21 expression increased with AAA development and was most prominent in the medial region of the diseased aorta (Fig. 1C).

We assessed known miR-21 target genes and found that the *Pten* gene was significantly down-regulated in placebo and nicotine-supplemented mice with elastase-induced AAA at all three time points versus sham-treated animals ($P < 0.05$; Fig. 1D). The *Pdcd4* and *Spry1* genes were significantly down-regulated at day 14 after infusion of elastase ($P < 0.05$; Fig. 1, E and F); however, the proapoptosis gene *Bcl2* was significantly up-regulated after 28 days ($P < 0.05$; Fig. 1G). Of the four validated target genes of miR-21 we tested, only *Pten* was differentially regulated (14 and 28 days after elastase infusion) in mice supplemented with nicotine compared to placebo-supplemented animals (Fig. 1D). The expression of miR-21 and its target gene *Pten* did not change in the unaffected suprarenal abdominal aortic segment of mice with AAA (fig. S1B).

Nicotine regulates *PTEN* activity via miR-21

Given the importance of various vascular cell types in AAA development and to confirm that miR-21 expression is also up-regulated in human aortic cell subtypes, we performed in vitro experiments using primary human aortic endothelial cells (hAECs), human aortic smooth muscle cells (hASMCs), and human aortic fibroblasts (hAFBs).

Cells were supplemented for 48 hours with vehicle or 10 nM (1.6 ng/ml) nicotine hydrogen tartrate salt, leading to nicotine concentrations comparable to those present in the vascular tissue of medium to heavy smokers (16). Before nicotine supplementation, miR-21 was robustly expressed in hASMCs and to a lesser extent in hAFBs, whereas in hAECs, miR-21 expression was almost nondetectable. After nicotine supplementation, miR-21 was significantly up-regulated in all three cell types ($P < 0.05$; Fig. 2A). The *PTEN, PDCD4*, and *SPRY1* genes were significantly down-regulated in nicotine-supplemented hASMCs ($P < 0.05$; Fig. 2B) and hAFBs ($P < 0.05$; Fig. 2C), but not in hAECs (fig. S1C); *BCL2* was significantly up-regulated only in nicotine-supplemented hAECs ($P < 0.05$; fig. S1C). In hASMCs, miR-21 was the highest up-regulated miRNA of those reported to target *PTEN* (fig. S5C).

We modulated miR-21 using either an antagomir (anti-21) to inhibit expression or a pre-miR (pre-21) to enhance expression in all three nicotine-supplemented cell types. Successful transfection (>50%of all cells) was confirmed by visual fluorescence microscopic analysis and fluorescence-activated cell sorting (FACS) for the fluorescent tag. Modulation ofmiR-21 expression affected *PTEN, PDCD4*, and *SPRY1* expression in hASMCs and hAFBs, whereas *BCL2* expression was not significantly regulated in any of the three cell types (Fig. 2, B and C, and fig. S1C).

Both cell proliferation assays using the MTT [3-(4,5--dimethylthiazol-2-yl)-2,5-diphenyltetrazolium bromide] dye and FACS analysis to measure apoptosis through detection of annexin V–positive cells revealed a key role for miR-21 in hASMCs. Cells transfected with anti-21 displayed less proliferation but a greater degree of apoptosis after nicotine supplementation when compared to those transfected with scrambled control miR (scr-miR); by contrast, enhanced miR-21 expression with pre-21 caused a marked increase in proliferation and decreased apoptosis when compared to the effects of scr-miR (Fig. 2, D and E).

Nicotine, interleukin-6, and angiotensin II regulate miR-21 expression

Nicotine is known to regulatemiR-21 expression through nuclear factor κB (NF-κB)–dependent modulation in cultured gastric cancer cells (17). Further, the miR-21 promoter contains a known NF-κB bindingsite (18). Given the inflammatory nature of AAA disease, we investigated the role of this pathway in the induction of miR-21 in hASMCs by supplementing cells with nicotine, interleukin-6 (IL-6), or angiotensin II. All three treatment regimens significantly enhanced miR-21 expression compared to untreated control cells ($P < 0.05$). These effects were significantly diminished by previous transfection of hASMCs with small interfering RNAs (siRNAs) to knock down either RELA (p65) or NFKB1 (p50), which are key components of the NF-κB signaling pathway (Fig. 2F and fig. S2, A and B). Successful knockdown of p50 and p65 (>75%) was verified by qRT-PCR and an assay to measure NF-κB activity (17) in siRNA-transfected and control hASMCs cells. The effects of modulating NF-κB activity and subsequent miR-21 regulation were most prominent in nicotine-supplemented hASMCs (Fig. 2F), and to a lesser extent in cells stimulated with IL-6 and angiotensin II (fig. S2, A and B).

In vivo modulation of miR-21 alters *Pten* expression and aneurysm progression

We used fluorescein isothiocyanate (FITC)–labeled locked nucleicacid (LNA)–anti–miR-21 to block miR-21 expression (anti-21), or lentivirus with pre-miR-21 that coexpresses green fluorescent protein (GFP) (lenti–premiR-21; pre-21) to perform gain-of-function studies. Double immunofluorescence staining confirmed that both anti-21 and pre-21 were successfully incorporated into the aortic wall. Both miR-21 modulators were coexpressed with the ASMC marker smooth muscle α-actin (SMA) (Fig. 3A). However, visualization of miR-21 modulators was almost exclusively limited to the site of injury, that is, the aneurysmal part of the abdominal aorta in mice infused with elastase (PPE model). In suprarenal aortic segments from mice in which miR-21 was up- or down-regulated, green fluorescence appeared to be largely due to autofluorescence from the elastic fibers. Except for the elastic layer, discrete fluorescent signal was detected only in the adventitial part of the suprarenal aorta, possibly delivered through the network of small vessels supplying large vessels like the aorta, known as vasa vasorum (Fig. 3A). In pre-21–transduced mice, miR-21measured via a GFP label was clearly detectable in what appeared to be a region of increased neointimal formation, an effect previously reported for modulation of miR-21 in other models of vascular disease (8).

Anti-21 treatment resulted in altered *Pten* mRNA levels at days 7 and 14 after elastase infusion compared to the scr-miR (Fig. 3B). *Pten* expression in anti-21–treated mice returned essentially to the levels found in sham mice (infused with saline) at both time points, indicating effective inhibition of miR-21 expression. After 28 days, *Pten* expression levels decreased in anti-21–treated mice, such that there was no longer a significant difference between anti-21– and scr-miR–treatedmice, suggesting that the effect of the single tail vein injection of LNA (10 mg/kg) had waned. We also observed similar trends in *Pten* expression in animals treated with anti-21 and nicotine (fig. S2C).

In contrast, treatment with lenti–pre-miR-21 [7.6×10^7 infectious units (IFUs)/ml] in mice infused with elastase led to further downregulation of *Pten* at 7, 14, and 28 days after tail

vein injection compared to sham-treated control mice and control mice infused with elastase and injected with an empty vector control (Fig. 3B). Again, similar effects on *Pten* mRNA levels were detected in nicotine-supplemented animals (fig. S2C).

Successful inhibition and overexpression of miR-21 in vivo were confirmed by qRT-PCR measurements of miR-21 expression in anti-21–and pre-21–transduced mice with AAA compared with control mice with AAA treated with a scr-miR or an empty vector control (fig. S2D).

Analogous to the direct immunofluorescence staining results, anti-21 or pre-21 treatment had minimal impact on *Pten* gene expression in the suprarenal (non-aneurysmal) abdominal aorta (fig. S1B). Only in the aneurysmal tissue of pre-21–transfected animals was *Pten* expression decreased compared with sham-treated control mice. However, no difference in *Pten* expression levels could be detected for pre-21 versus empty vector or anti-21 versus scrambled miRNA in the suprarenal aorta, again suggesting that only at the site of injury did sufficient uptake of miR-21 modulators occur.

Inhibition (with the LNA antagomir) of miR-21 after elastase infusion greatly augmented AAA growth, whereas overexpression with pre-21 inhibited AAD expansion (from days 7 to 28) (Fig. 3C and table S4). These results were replicated in nicotine-supplemented animals (fig. S2E). Three mice that received both nicotine and anti-21 died (at 11, 15, and 19 days) due to rupture of massively enlarged AAAs, an extremely uncommon event in the elastase-induced aneurysm model when using 10-week-old male C57BL/6 mice.

Staining with Picrosirius Red demonstrated the substantial structural impact of treatment with anti-21 and pre-21 (versus a scrambled miRNA) 14 days after elastase-induced AAA development (Fig. 3D). Obvious aortic wall thickening due to smooth muscle proliferation was visible in the AAA of mice receiving scrambled miRNA compared with saline-infused controls (sham). This process was much more prominent in mice injected with pre-21 compared with the other groups (anti-21, scrambled miRNA, sham); almost no wall thickening or smooth muscle cell proliferation could be detected in the aortas of anti-21–treatedmice (Fig. 3E). The aortic diameters of the latter were greatly enlarged (Fig. 3, C and D).

The results for differentially regulated *Pten* gene expression were confirmed at the protein level by Western blot for PTEN and its downstream targets phospho-AKT (p-AKT) and AKT in mice treated with elastase alone or elastase plus nicotine that received anti-21 or pre-21 (Fig. 4, A and B).

Differentially expressed miR-21 affects proliferation, apoptosis, and inflammation

Immunohistochemical analysis of PTEN, Ki-67 (a neutral marker of cell proliferation), and caspase-3 (an apoptosis marker) was performed to illustrate the regulation of cell proliferation and apoptosis as a consequence of modulating miR-21 and PTEN activity. Cell proliferation measured by Ki-67–positive cells correlated negatively with PTEN expression, whereas cell apoptosis measured by the number of caspase-3–positive cells correlated

positively with PTEN expression (Fig. 4, C and D). By contrast, miR-21 did not alter the fibrotic response to aneurysm development (fig. S5, A and B).

Immunohistochemical staining for Mac-1 demonstrated enhanced monocyte/macrophage activation in animals treated with elastase and nicotine (Fig. 5, A and B). This was further confirmed by qRT-PCR results showing that the expression of downstream target genes of the *Pten*/mTOR inflammatory pathway [monocyte chemotactic protein-1 (*Mcp1*), IL-6 (*Il6*), stromal cell–derived factor-1 (*Cxcl12*), and chemokine C-X-C motif ligand 1 (*Cxcl1*)] was increased in nicotine-supplemented elastase-infused mice (Fig. 5C). It has been established that miR-21 expression correlates with expression of these inflammatory markers and regulators, and with the expression of *Mmp2* (19). We found that pre-21 treatment (which boosts miR-21 expression) increased the expression of *Il6* and *Mcp1* in elastase-induced AAAs compared with a scr-miR but had no effect on *Mmp2* expression (Fig. 5D).

miR-21 and *Pten* regulate AAA expansion

We used a second established model of aneurysm formation, the angiotensin II infusion model in 10-week-old mice that lack apolipoprotein E (apoE) (20), to confirm that regulation of miR-21 and *Pten* is not exclusive to the elastase infusion model of AAA. miR-21 expression was up-regulated in angiotensin II–infused animals compared with a saline-infused control group after 14 and 28 days. As in the elastase infusion model, miR-21 was further up-regulated in nicotine-supplemented animals at both time points (Fig. 6A). *Pten* expression was decreased in angiotensin II–infused mice, with further down-regulation at both time points when these animals were treated with nicotine (Fig. 6B). AAD was increased in the nicotine group from days 7 to 28 compared with animals infused with angiotensin II only or saline control (Fig. 6C and table S5). The mortality rate over the time course, because of dissection and rupture of the aorta, was higher in animals treated with angiotensin II and nicotine (60%) when compared with animals infused with angiotensin II alone (30%; $P < 0.01$).

In loss-of-function studies using anti-21, *Pten* expression was increased (Fig. 6D), resulting in augmented development and progression of AAA 28 days after initiation of angiotensin II infusion (Fig. 6E and table S6). Gain-of-function studies using pre-21 caused a decrease in *Pten* expression, limiting AAA expansion after 14 and 28 days compared with scrambled miRNA, empty vector, and anti-21 treatments (Fig. 6, D and E). Picrosirius Red–stained images from day 28 demonstrated differences in proliferation and composition of the vascular wall in mice where miR-21 expression was modulated (fig. S3, A and B). The mortality rate due to aortic rupture throughout the 28-day follow-up period was increased in anti-21–injected mice (80%) compared with those receiving a scr-miR (33%; $P < 0.01$), an empty vector control (30%; $P < 0.01$), or pre-21, which boosted expression of miR-21 (20%; $P < 0.01$). However, miR-21 expression was regulated to a lesser extent in the angiotensin II model compared with the elastase-induced model of AAA formation (fig. S3C). Accordingly, changes in AAA were less prominent in the former compared to the latter mouse model.

miR-21 expression is altered in human AAA disease

Human aortic samples from patients with AAA who underwent surgical repair of an enlarged abdominal aorta (57 to 68 mm) corroborated our findings of up-regulated miR-21 expression and decreased PTEN expression in the aneurysm. We compared a group of frequent and active smokers (n = 8; mean consumption, 37 ± 18 pack-years; mean age, 63 ± 9 years) to a group of patients who had never smoked (n=5; mean age, 66 ± 10 years), all with AAA. According to hospital documentation, all 13 patients were on similar medical therapy, potentially influencing their aortic molecular milieu (statin therapy plus β-blockers, either angiotensin receptor blocker or angiotensin-converting enzyme inhibitors), at the time of surgical intervention. All patients were male, of Caucasian descent, and nondiabetic. qRT-PCR revealed that miR-21 expression in diseased aortic tissue was 6.7 ± 1.1 (SEM)–fold up-regulated in nonsmokers with AAA, and 12.8 ± 2.1 (SEM)–fold up-regulated in smokers with AAA, when compared with normal abdominal aortic tissue from a group of organ donor patients without AAA ($P < 0.05$; n = 5; mean age, 33 ± 14 years) at time of explantation (n = 3 heart; n = 2 kidney). In the same group of patients, PTEN was down-regulated [2.4 ± 0.5 (SEM)–fold in AAA nonsmokers; 4.3 ± 1.2 (SEM)–fold in AAA smokers] compared to control patients ($P < 0.05$; Fig. 6F).

DISCUSSION

Despite tremendous efforts using traditional approaches to reduce the mortality and morbidity of AAA disease, the identification of the underlying causes as well as appropriate medical intervention remain a major clinical challenge. New approaches in understanding and fighting AAA are needed. Because of the complex pathological mechanisms of aneurysm development, progression, and rupture, the standard methods of designing drugs to target specific enzymes, cell surface receptors, or single proteins are unlikely to be sufficient. In this dismaying scenario, the discovery of an entirely new method of gene regulation through miRNAs, and their validation as markers and modulators of vascular remodeling in pathological conditions, provides new therapeutic pathways for developing innovative therapies. In rodent models, modulation of miRNAs has proven to be successful in limiting and treating heart failure (10, 21), myocardial ischemia, and infarction (22) with subsequent cardiac fibrosis (23), enhancing angiogenesis in peripheral artery disease (24, 25), and limiting myointimal hyperplasia/restenosis in vascular injury (8, 26). Previous studies have already indicated that cigarette smoke exposure can augment AAA growth in the elastase infusion mouse model of AAA (27, 28). We present data showing that nicotine supplementation also leads to significant AAA expansion in two different mouse models of aneurysm disease. The results of our study suggest that not only cigarette smoke but potentially also the consumption of other forms of nicotine, like chewing tobacco or snuff (as well as nicotine patches, which are widely used for smoking cessation), may increase risk for AAA development and progression. Unfortunately, human data for the incidence and prevalence of AAA disease in relation to forms of nicotine uptake other than active firsthand cigarette smoke are currently lacking.

The fact that overexpression of a single miRNA, miR-21, in our study can induce cellular proliferation within the aortic wall and thereby protect mice from AAA expansion indicates

the power of individual miRNAs for coordinating expression of target genes involved in complex physiological and disease phenotypes. The key difference between modulating miRNAs and traditional therapeutic approaches is that most drugs have specific cellular targets, whereas miRNAs can potentially modulate entire functional gene networks. However, this can also be considered a limitation because unintended side effects may occur.

The therapeutic goal is generally to reverse or arrest pathological changes resulting from disease. One would predict that miRNAs found to be up-regulated in pathological conditions should be knocked down by antagomirs, and those down-regulated should be supplemented by treatment with pre-miRNAs or miRNA mimics to treat disease. Our studies suggest a different scenario with regard to AAA development and progression. The data suggest that up-regulation of miR-21 is a physiological response to aortic expansion. This protective response may be augmented when deleterious stimuli such as nicotine are present. Although this endogenous pathway may be insufficient to abrogate aortic expansion, our data indicate that it remains a potential therapeutic target.

Modulation of miR-21 in AAA disease as a protective physiological response follows a common pattern in cardiovascular diseases. For example, natriuretic peptides (such as brain natriuretic peptide) are released from the left ventricle of the heart when high filling pressures occur. Their primary purpose is to inhibit volume overload and to preserve cardiac function (29). AAA development leads to increased miR-21 expression and decreased PTEN expression and results in a pro-proliferative and antiapoptotic response of smooth muscle cells within the vessel wall, most likely in an attempt to protect the aorta from further expansion and ultimate rupture (fig. S6). This appeared to be the case in the two types of murine AAA models we investigated, as well as representative human AAA samples.

Inhibition of the PTEN/PI3K/AKT signaling pathway by miR-21 was instrumental in limiting AAA expansion, a mechanism that was particularly evident when miR-21was overexpressed through treatment with pre-21. Further, the pro-proliferative effects of down-regulated PTEN were diminished by treatment with anti-21, blocking miR-21 up-regulation, and leading to a marked acceleration of AAA development and even rupture in nicotine-supplemented animals.

Previous studies have indicated that after an early phase of recruitment and activation of inflammatory cells in the elastase-infused model of AAA (until 7 days after infusion), stabilization of vascular integrity becomes the most important factor in limiting aneurysm expansion (between days 7 and 14) (30, 31). The critical role of smooth muscle cell apoptosis and depletion in human aneurysmal tissues has previously been reported (32). In addition to compromising vascular wall structure, loss of smooth muscle cells eliminates a cell population capable of directing connective tissue repair and vessel wall stabilization. In vivo as well as in vitro data presented in the current study indicate that smooth muscle cell proliferation and apoptosis are highly affected by altered expression of miR-21.

Our in vitro studies have also identified the transcription factor NF-κB as a crucial positive regulator of miR-21 expression in vascular cells. Nicotine, IL-6, and angiotensin II were each able to induce miR-21 through up-regulation of NF-κB. Although inhibition of NF-κB

using siRNAs against its subunits or direct drug targeting is well established in vitro, it remains impractical for translational approaches in humans because of the wide variety of functions of NF-κB and the many cellular processes in which this master transcription factor is involved (33). Although this is also an issue with miRNAs, modulation of miR-21 appears to be a more feasible approach to balancing disease-determining mechanisms such as proliferation and apoptosis in the aortic wall. Additionally, inhibition of NF-κB in vivo would be expected to decrease miR-21 levels, an effect our data suggest could worsen outcomes.

A proinflammatory pattern of gene expression (*Mcp1, Il6, Cxcl1*, and *Cxcl12*) was more evident in nicotine-supplemented compared to placebo-supplemented mice with AAAs after elastase infusion. Accordingly, the number of Mac-1–positive cells, an indicator of macrophage infiltration and inflammatory activity, was much higher in the nicotine-treated cohort. Furthermore, *Mmp2* expression was elevated in mice treated with elastase and nicotine compared with mice treated with elastase alone or sham-treated animals (fig. S3D). This may be partially responsible for the larger aneurysms observed in the nicotine group. The effect was accompanied by a corresponding increase in miR-21 expression and smooth muscle cell proliferation in the vessel wall, presumably a protective response. Overexpression of miR-21 induced by treatment with pre-21 increased expression of some proinflammatory genes 14 days after AAA induction by elastase infusion (*Il6* and *Mcp1*; Fig. 5D). Proinflammatory activity was increased in pre-21–transduced mice compared to those treated with anti-21, scrambled miRNA, or sham-operated mice (fig. S4A). However, this did not result in further expansion of aneurysms, most likely because of acceleration of the proproliferative response in animals with augmented miR-21 expression (Fig. 3, D and E, and figs. S3, A and B, and S4B).

The methods of anti-21 and pre-21 administration used in this study are limited in application by their systemic effects on other organ systems, in particular the heart and liver, which intravenous therapies often affect to a greater extent than the aorta. In pre-21–treated animals, *Spry1* and *Pten* were down-regulated in heart and liver tissue samples (fig. S4, C and D), an effect that in previous studies led to cardiac fibrosis with subsequent heart failure (9, 10), as well as liver fibrosis and development of hepatocellular carcinoma (34, 35). In contrast, anti-21 treatment, which in our hands causes marked AAA progression, potentially may provide protective effects to combat cardiac fibrosis and heart failure, as well as fibrosis and tumor formation in the liver. These findings suggest that systemic up-regulation of miR-21 will not be useful as a translational approach to treat AAA in human patients. However, local delivery with expandable balloons or drug-eluting stent grafts containing pre-21 miRNAs may emerge as a promising tool to trigger proliferation in the aortic wall in human patients with AAA disease. Experimental delivery of siRNA molecules eluted from stents or delivered with balloons has already been shown to be efficacious (36).

Direct delivery of LNA–anti-miRNAs to block the expression of a particular miRNA resembles pharmacological intervention, and there have been no immunogenic safety or toxicity issues reported thus far (37). However, a major drawback for long-term use in chronic diseases such as AAA is the necessity of repeated dosing required for effective treatment. In our study, the effects of LNA–anti–miR-21 diminished after 28 days, having no

further impact on miR-21 target gene expression. LNA–anti-miRNA administration of other miRNAs could have limited use if the route of delivery requires an invasive procedure.

The second approach used in our experiments is vascular gene therapy. A lentiviral vector, derived from HIV-1, appears to be an effective tool to deliver pre-miR-21 to the diseased aorta. The main safety concern with lentiviral vectors is that homologous recombination may produce wild-type HIV. However, the engineering of new lentiviruses, such as that used in our study, where the U3 promoter region of the long terminal repeats is deleted (leading to a self-inactivating lentivirus) resolves this issue, making them a promising vector for future application in gene therapy for treating cardiovascular diseases (38). This approach may simplify the delivery of not only pre-miRNA and miRNA mimics but also antagomirs because of the small size of miRNA coding sequences. This would also make drug-mediated regulation of expression feasible. A detailed understanding of the biology of miRNAs and optimization of gene delivery vectors will determine the future of therapeutic miRNAs and their application in treating cardiovascular diseases such as AAA.

MATERIALS AND METHODS

Mice

All animal protocols were approved by the Administrative Panel on Laboratory Animal Care at Stanford University (http://labanimals.stanford.edu/) and followed the National Institutes of Health and U.S. Department of Agriculture *Guidelines for Care and Use of Animals in Research*. All experiments were performed with 10-week-old male C57BL/6 (PPE model) and 10-week-old male apoE$^{-/-}$ mice on a C57BL/6 background (angiotensin II infusion model). Animals were purchased from The Jackson Laboratory.

PPE infusion model

PPE infusion AAA induction techniques were performed as previously described (39). Details on the operative procedure as well as survival rate are described in the Supplementary Material.

Angiotensin II infusion model

Osmotic pumps (model 2004, Alzet) containing either angiotensin II (1 μg/kg perminute, Sigma-Aldrich) or saline were introduced in 10-weekold apoE$^{-/-}$ male mice (C57BL/6J background) as previously described (40). A more detailed description can be found in the Supplementary Material.

Nicotine and placebo pellet implantation

Pellets containing 5 mg of nicotine with a 60-day release (release rate of 2.2 mg/kg per day) or placebo (both purchased from Innovative Research of America) were implanted subcutaneously on the lateral side of the neck/shoulder region 7 days before aneurysm induction with PPE or angiotensin II. Pellets were implanted with a stainless steel reusable precision trochar (Innovative Research of America) with regular medical point needle and rounded stylet.

Cotinine concentration measurements

Cotinine (degradation product of nicotine) concentration was measured (ng/ml) in serum of nicotine-treated mice ($n = 3$ for each time point) by enzyme-linked immunosorbent assay (ELISA) (Calbiotech) 24 hours and 7, 14, and 28 days after pellet implantation according to the manufacturer's instructions.

Blood pressure measurements

Systolic and diastolic blood pressures in conscious mice were measured with a computerized, noninvasive tail-cuff and infrared pulse detection system (Visitech Systems Inc.) according to an established protocol (41) and the manufacturer's instructions. Detailed information on the procedure can be found in the Supplementary Material.

Aortic diameter measurements by ultrasound imaging

At baseline and 3, 7, 14, 21, and 28 days after aneurysm induction, B-mode ultrasound imaging was performed on the operated mice to assess the AAD as previously described (42). For detailed information, see the Supplementary Material.

Histological and immunohistochemical analysis

Standardized protocols were used as previously described (42). Details are found in the Supplementary Material.

Western blot analysis

Protein extraction and Western blot analysis were performed with established methodology (41). The antibodies used were the same as those used for immunohistochemical analysis (see the Supplementary Material).

RNA quantification

Total RNA was isolated with a TRIzol-based (Invitrogen) RNA isolation protocol. RNA was quantified by NanoDrop (Agilent Technologies), and RNA and miRNA quality were verified with the Agilent 2100 Bioanalyzer (Agilent Technologies). Samples required 260/280 ratios of >1.8 and sample RNA integrity numbers of ≥9 for inclusion. RNA was reverse-transcribed with the TaqMan MicroRNA Reverse Transcription kit (Applied Biosystems) according to the manufacturer's instructions. Further details are described in the Supplementary Material.

In situ hybridization

ISH for miR-21 was performed with the miRCURY LNA microRNA ISH Optimization Kit (Exiqon) and 5′-digoxigenin (DIG)–labeled probes for mmu-miR-21 according to the manufacturer's protocol. The sequence of the LNA miR-21 control probe was 5′-DIG/TCAACATCAGTCTGATAAGCTA/DIG-3′. LNA scr-miR sequence was 5′-DIG/GTGTAACACGTCTATACGCCCA/DIG-3′.

LNA–anti–miR-21 injection

Either anLNA–anti–miR-21 or a scr-miR (miRCURY LNA microRNA inhibitor from Exiqon) was injected via tail vein under pressure [in 1 ml of phosphate-buffered saline (PBS) over 5 to 10 s]. The concentration of anti-miR or scrambled miR was 10 mg/kg. A single injection of anti-miR was performed 1 day after AAA induction of both mouse models. The custom-made LNA–anti–miR-21 5′-3′ sequence was TCAGTCTGATAAGCT. The LNA scr-miR 5′-3′ sequence was ACGTCTATACGCCCA.

Lenti–pre-miR-21 injection

The hsa–miR-21 pre-miR construct (System Biosciences) was cloned into an HIV lentiviral vector containing a co-GFP reporter and with the miR precursor under constitutive cytomegalovirus promoter control. The precursor miR-21 sequence was TGTCGGGTAGCTTATCAGACTGATGTTGACTGTTGAATCTCATGGCAACACCAGATGGGCTGTCTGACA. Lenti–pre-miR-21 was injected via tail vein in 1 ml of PBS with 7.6×10^7 IFUs of loaded lentivirus per mouse. Lenti–pre-miRs were injected 1 day after AAA induction.

Double immunofluorescence studies

Primary antibody for GFP was applied after washing with 10% PBS with conventional immunohistochemical dilutions (Supplementary Materials and Methods). Secondary antibodies were replaced with goat anti-rabbit antibodies labeled with Alexa Fluor (Invitrogen; dilution 1:250) dye with a maximum excitation at 488 nm (green). Polyclonal rabbit SMA primary antibody was detected with a goat anti-mouse secondary antibody labeled red with Alexa Fluor 568 (Invitrogen). Images were obtained and analyzed by fluorescence microscopy (microscope and camera from Nikon).

In vitro studies

hASMCs, hAFBs, and hAECs were propagated in growth media [SmGM-2 (for hASMCs), SCBM (for hAFBs), and EBM-2 (for hAECs)] with 5% fetal bovine serum as per the manufacturer’s instructions (Lonza, passages 4 to 5). Subconfluent (~80%) plates were treated with 10 nM (−)-nicotine hydrogen tartrate salt (Sigma-Aldrich) for 24 hours and subsequently harvested for RNA analysis. Further details on transfection of cultured cells, proliferation/cell survival, and apoptosis assays are described in detail in the Supplementary Materials.

Human sample acquisition and preparation

Approval for studies on human tissue samples was obtained under informed consent and according to the declaration of Helsinki. Human samples from patients who underwent surgical repair of their AAA, as well as abdominal aortic samples from organ donors, were harvested during surgery (or explantation), snap-frozen, and stored at −80°C before processing for RNA analysis.

Statistics

Data are presented as means ± SEM. Groups were compared with Student's *t* test for parametric data. When comparing multiple groups, data were analyzed by analysis of variance (ANOVA) with Bonferroni's post test. Sequential measurements (AADs at consecutive time points) were analyzed by one-way repeated-measures ANOVA. A value of $P < 0.05$ was considered statistically significant.

Supplementary Material

Refer to Web version on PubMed Central for supplementary material.

Acknowledgments

We thank J. Chin, B. A. Dake, N. Kimura, H. Kosuge, and T. Kitagawa for expert technical assistance.

Funding: This work is supported by research grants from the NIH (1P50HL083800-01 to P.S.T., R.L.D., and M.V.M.; 5K08 HL080567 to J.M.S.), the California Tobacco Related Disease Research Program of the University of California (18XT-0174 to P.S.T.), the Deutsche Forschungsgemeinschaft (MA4688/1-1 to L.M.), the American Heart Association (09POST2260118 to L.M.), and the Deutsche Herzstiftung e.V. (S/02/11 to D.R.M.).

REFERENCES AND NOTES

1. Fleming C, Whitlock EP, Beil TL, Lederle FA. Screening for abdominal aortic aneurysm: A best-evidence systematic review for the U.S. Preventive Services Task Force. Ann. Intern. Med. 2005; 142:203–211. [PubMed: 15684209]
2. Creager MA, Jones DW, Easton JD, Halperin JL, Hirsch AT, Matsumoto AH, O'Gara PT, Safian RD, Schwartz GL, Spittell JA. American Heart Association, Atherosclerotic Vascular Disease Conference: Writing Group V. Medical decision making and therapy. Circulation. 2004; 109:2634–2642. [PubMed: 15173046]
3. Powell JT, Worrell P, MacSweeney ST, Franks PJ, Greenhalgh RM. Smoking as a risk factor for abdominal aortic aneurysm. Ann. N. Y. Acad. Sci. 1996; 800:246–248. [PubMed: 8959002]
4. Weintraub NL. Understanding abdominal aortic aneurysm. N Engl. J. Med. 2009; 361:1114–1116. [PubMed: 19741234]
5. Lederle FA, Nelson DB, Joseph AM. Smokers' relative risk for aortic aneurysm compared with other smoking-related diseases: A systematic review. J Vasc. Surg. 2003; 38:329–334. [PubMed: 12891116]
6. van Rooij E. The art of microRNA research. Circ. Res. 2011; 108:219–234. [PubMed: 21252150]
7. Krichevsky AM, Gabriely G. miR-21: A small multi-faceted RNA. J Cell. Mol. Med. 2009; 13:39–53. [PubMed: 19175699]
8. Ji R, Cheng Y, Yue J, Yang J, Liu X, Chen H, Dean DB, Zhang C. MicroRNA expression signature and antisense-mediated depletion reveal an essential role of microRNA in vascular neointimal lesion formation. Circ. Res. 2007; 100:1579–1588. [PubMed: 17478730]
9. Roy S, Khanna S, Hussain SR, Biswas S, Azad A, Rink C, Gnyawali S, Shilo S, Nuovo GJ, Sen CK. MicroRNA expression in response to murine myocardial infarction: miR-21 regulates fibroblast metalloprotease-2 via phosphatase and tensin homologue. Cardiovasc. Res. 2009; 82:21–29. [PubMed: 19147652]
10. Thum T, Gross C, Fiedler J, Fischer T, Kissler S, Bussen M, Galuppo P, Just S, Rottbauer W, Frantz S, Castoldi M, Soutschek J, Koteliansky V, Rosenwald A, Basson MA, Licht JD, Pena JT, Rouhanifard SH, Muckenthaler MU, Tuschl T, Martin GR, Bauersachs J, Engelhardt S. MicroRNA-21 contributes to myocardial disease by stimulating MAP kinase signalling in fibroblasts. Nature. 2008; 456:980–984. [PubMed: 19043405]

11. Liu X, Cheng Y, Yang J, Krall TJ, Huo Y, Zhang C. An essential role of PDCD4 in vascular smooth muscle cell apoptosis and proliferation: Implications for vascular disease. Am. J. Physiol. Cell Physiol. 2010; 298:C1481–C1488. [PubMed: 20357187]
12. Oudit GY, Penninger JM. Cardiac regulation by phosphoinositide 3-kinases and PTEN. Cardiovasc. Res. 2009; 82:250–260. [PubMed: 19147653]
13. Bunney TD, Katan M. Phosphoinositide signalling in cancer: Beyond PI3K and PTEN. Nat. Rev. Cancer. 2010; 10:342–352. [PubMed: 20414202]
14. Lee J, Cooke JP. The role of nicotine in the pathogenesis of atherosclerosis. Atherosclerosis. 2011; 215:281–283. [PubMed: 21345436]
15. Barua RS, Ambrose JA, Eales-Reynolds LJ, DeVoe MC, Zervas JG, Saha DC. Heavy and light cigarette smokers have similar dysfunction of endothelial vasoregulatory activity: An in vivo and in vitro correlation. J Am. Coll. Cardiol. 2002; 39:1758–1763. [PubMed: 12039488]
16. Wang Z, Wu W, Fang X, Wang Y, Xiao C, Zhao R, Wang L, Qiao Z. Protein expression changed by nicotine in rat vascular smooth muscle cells. J Physiol. Biochem. 2007; 63:161–169. [PubMed: 17933390]
17. Shin VY, Jin H, Ng EK, Cheng AS, Chong WW, Wong CY, Leung WK, Sung JJ, Chu KM. NF-κB targets miR-16 and miR-21 in gastric cancer: Involvement of prostaglandin E receptors. Carcinogenesis. 2011; 32:240–245. [PubMed: 21081469]
18. Zhou R, Hu G, Gong AY, Chen XM. Binding of NF-κB p65 subunit to the promoter elements is involved in LPS-induced transactivation of miRNA genes in human biliary epithelial cells. Nucleic Acids Res. 2010; 38:3222–3232. [PubMed: 20144951]
19. Furgeson SB, Simpson PA, Park I, Vanputten V, Horita H, Kontos CD, Nemenoff RA, Weiser-Evans MC. Inactivation of the tumour suppressor, PTEN, in smooth muscle promotes a pro-inflammatory phenotype and enhances neointima formation. Cardiovasc. Res. 2010; 86:274–282. [PubMed: 20051384]
20. Daugherty A, Cassis LA. Mouse models of abdominal aortic aneurysms. Arterioscler. Thromb. Vasc. Biol. 2004; 24:429–434. [PubMed: 14739119]
21. Duisters RF, Tijsen AJ, Schroen B, Leenders JJ, Lentink V, van der Made I, Herias V, van Leeuwen RE, Schellings MW, Barenbrug P, Maessen JG, Heymans S, Pinto YM, Creemers EE. miR-133 and miR-30 regulate connective tissue growth factor: Implications for a role of microRNAs in myocardial matrix remodeling. Circ. Res. 2009; 104:170–178. [PubMed: 19096030]
22. Hu S, Huang M, Li Z, Jia F, Ghosh Z, Lijkwan MA, Fasanaro P, Sun N, Wang X, Martelli F, Robbins RC, Wu JC. MicroRNA-210 as a novel therapy for treatment of ischemic heart disease. Circulation. 2010; 122:S124–S131. [PubMed: 20837903]
23. van Rooij E, Sutherland LB, Thatcher JE, DiMaio JM, Naseem RH, Marshall WS, Hill JA, Olson EN. Dysregulation of microRNAs after myocardial infarction reveals a role of miR-29 in cardiac fibrosis. Proc. Natl. Acad. Sci. U.S.A. 2008; 105:13027–13032. [PubMed: 18723672]
24. Fish JE, Santoro MM, Morton SU, Yu S, Yeh RF, Wythe JD, Ivey KN, Bruneau BG, Stainier DY, Srivastava D. miR-126 regulates angiogenic signaling and vascular integrity. Dev. Cell. 2008; 15:272–284. [PubMed: 18694566]
25. Bonauer A, Carmona G, Iwasaki M, Mione M, Koyanagi M, Fischer A, Burchfield J, Fox H, Doebele C, Ohtani K, Chavakis E, Potente M, Tjwa M, Urbich C, Zeiher AM, Dimmeler S. MicroRNA-92a controls angiogenesis and functional recovery of ischemic tissues in mice. Science. 2009; 324:1710–1713. [PubMed: 19460962]
26. Leeper NJ, Raiesdana A, Kojima Y, Chun HJ, Azuma J, Maegdefessel L, Kundu RK, Quertermous T, Tsao PS, Spin JM. MicroRNA-26a is a novel regulator of vascular smooth muscle cell function. J Cell. Physiol. 2011; 226:1035–1043. [PubMed: 20857419]
27. Buckley C, Wyble CW, Borhani M, Ennis TL, Kobayashi DK, Curci JA, Shapiro SD, Thompson RW. Accelerated enlargement of experimental abdominal aortic aneurysms in a mouse model of chronic cigarette smoke exposure. J Am. Coll. Surg. 2004; 199:896–903. [PubMed: 15555973]
28. Bergoeing MP, Arif B, Hackmann AE, Ennis TL, Thompson RW, Curci JA. Cigarette smoking increases aortic dilatation without affecting matrix metalloproteinase-9 and-12 expression in a modified mouse model of aneurysm formation. J Vasc. Surg. 2007; 45:1217–1227. [PubMed: 17398058]

29. Daniels LB, Maisel AS. Natriuretic peptides. J Am. Coll. Cardiol. 2007; 50:2357–2368. [PubMed: 18154959]
30. Thompson RW, Curci JA, Ennis TL, Mao D, Pagano MB, Pham CT. Pathophysiology of abdominal aortic aneurysms: Insights from the elastase-induced model in mice with different genetic backgrounds. Ann. N. Y. Acad. Sci. 2006; 1085:59–73. [PubMed: 17182923]
31. Van Vickle-Chavez SJ, Tung WS, Absi TS, Ennis TL, Mao D, Cobb JP, Thompson RW. Temporal changes in mouse aortic wall gene expression during the development of elastase-induced abdominal aortic aneurysms. J Vasc. Surg. 2006; 43:1010–1020. [PubMed: 16678698]
32. Thompson RW, Liao S, Curci JA. Vascular smooth muscle cell apoptosis in abdominal aortic aneurysms. Coron. Artery Dis. 1997; 8:623–631. [PubMed: 9457444]
33. Hayden MS, Ghosh S. Shared principles in NF-κB signaling. Cell. 2008; 132:344–362. [PubMed: 18267068]
34. Watanabe S, Horie Y, Kataoka E, Sato W, Dohmen T, Ohshima S, Goto T, Suzuki A. Nonalcoholic steatohepatitis and hepatocellular carcinoma: Lessons from hepatocyte-specific phosphatase and tensin homolog (PTEN)-deficient mice. J Gastroenterol. Hepatol. 2007; 22(Suppl. 1):S96–S100. [PubMed: 17567478]
35. Meng F, Henson R, Wehbe-Janek H, Ghoshal K, Jacob ST, Patel T. MicroRNA-21 regulates expression of the PTEN tumor suppressor gene in human hepatocellular cancer. Gastroenterology. 2007; 133:647–658. [PubMed: 17681183]
36. San Juan A, Bala M, Hlawaty H, Portes P, Vranckx R, Feldman LJ, Letourneur D. Development of a functionalized polymer for stent coating in the arterial delivery of small interfering RNA. Biomacromolecules. 2009; 10:3074–3080. [PubMed: 19761207]
37. Elmén J, Lindow M, Schütz S, Lawrence M, Petri A, Obad S, Lindholm M, Hedtjarn M, Hansen HF, Berger U, Gullans S, Kearney P, Sarnow P, Straarup EM, Kauppinen S. LNA-mediated microRNA silencing in non-human primates. Nature. 2008; 452:896–899. [PubMed: 18368051]
38. Mishra PK, Tyagi N, Kumar M, Tyagi SC. MicroRNAs as a therapeutic target for cardiovascular diseases. J Cell. Mol. Med. 2009; 13:778–789. [PubMed: 19320780]
39. Azuma J, Asagami T, Dalman R, Tsao PS. Creation of murine experimental abdominal aortic aneurysms with elastase. J Vis. Exp. 2009; 29:1280.
40. Goergen CJ, Azuma J, Barr KN, Magdefessel L, Kallop DY, Gogineni A, Grewall A, Weimer RM, Connolly AJ, Dalman RL, Taylor CA, Tsao PS, Greve JM. Influences of aortic motion and curvature on vessel expansion in murine experimental aneurysms. Arterioscler. Thromb. Vasc. Biol. 2011; 31:270–279. [PubMed: 21071686]
41. Chun HJ, Ali ZA, Kojima Y, Kundu RK, Sheikh AY, Agrawal R, Zheng L, Leeper NJ, Pearl NE, Patterson AJ, Anderson JP, Tsao PS, Lenardo MJ, Ashley EA, Quertermous T. Apelin signaling antagonizes Ang II effects in mouse models of atherosclerosis. J Clin. Invest. 2008; 118:3343–3354. [PubMed: 18769630]
42. Azuma J, Maegdefessel L, Kitagawa T, Dalman RL, McConnell MV, Tsao PS. Assessment of elastase-induced murine abdominal aortic aneurysms: Comparison of ultrasound imaging with in situ video microscopy. J Biomed. Biotechnol. 2011; 2011:252141. [PubMed: 21331328]

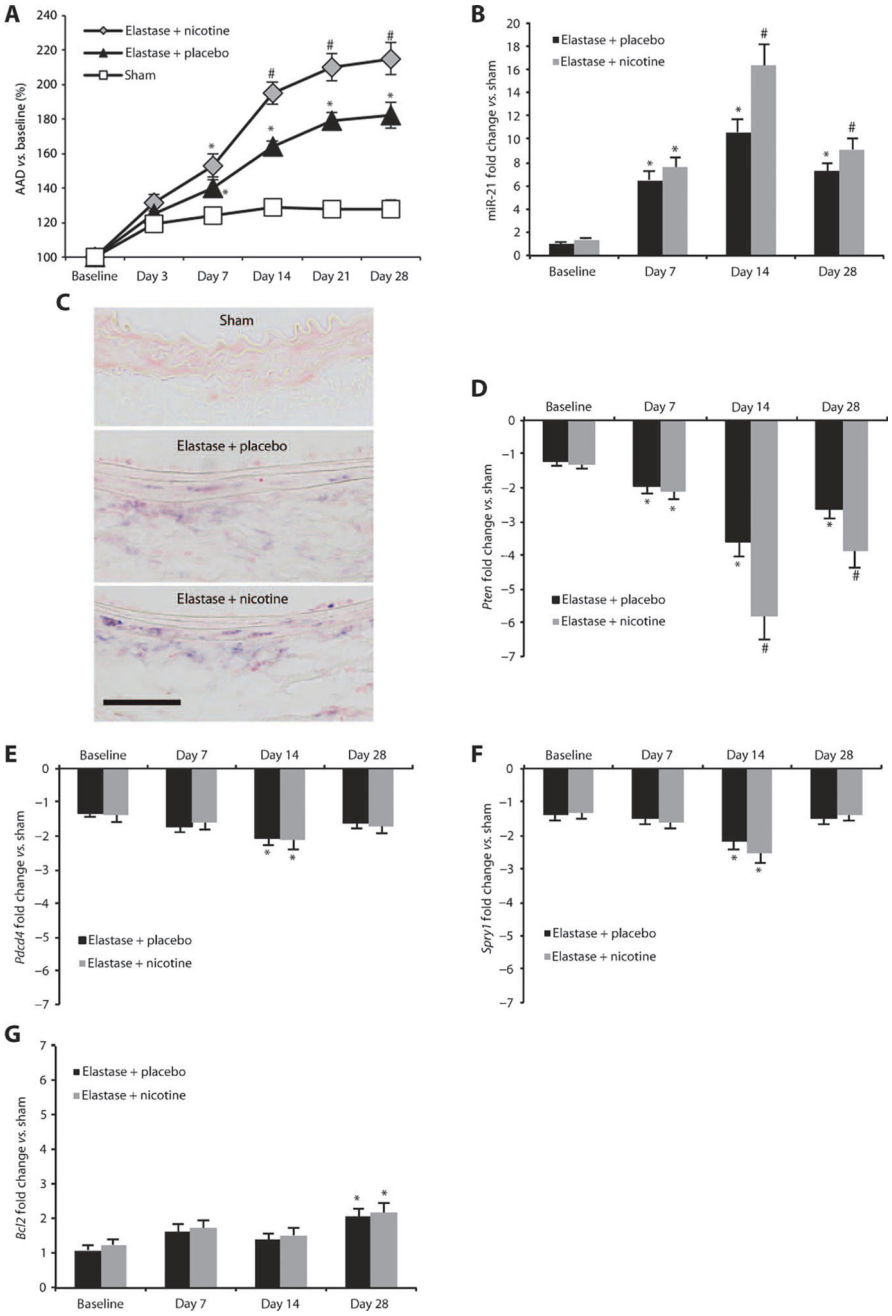

Fig. 1.

miR-21 and target gene expression in AAAs induced by elastase infusion. (**A**) AAD (versus baseline as a percentage) in elastase-infused mice supplemented with placebo and nicotine compared to saline-infused control mice (sham). (**B**) miR-21 expression in mice infused with elastase supplemented with placebo or nicotine compared to sham animals. (**C**) ISH staining formiR-21 (purple chromagen) in mice infused with elastase and supplemented with placebo, elastase-infused mice supplemented with nicotine, or saline-infused (sham) animals 14 days after AAA induction (labels on luminal side; scale bar, 50 μm). (**D** to **G**) mRNA expression for *Pten* (D), *Pdcd4* (E), *Spry1* (F), and *Bcl2* (G) genes in mice infused with

elastase and supplemented with either placebo or nicotine compared to sham animals. $n = 5$ to 8 for each treatment group and time point. Data are means ± SEM. $*P < 0.05$ versus sham; $\#P < 0.05$ versus elastase + placebo and sham. Level of significance was determined using one-way ANOVA with Bonferroni's post test. Sequential measurements (AADs at consecutive time points) were analyzed by one-way repeated-measures ANOVA.

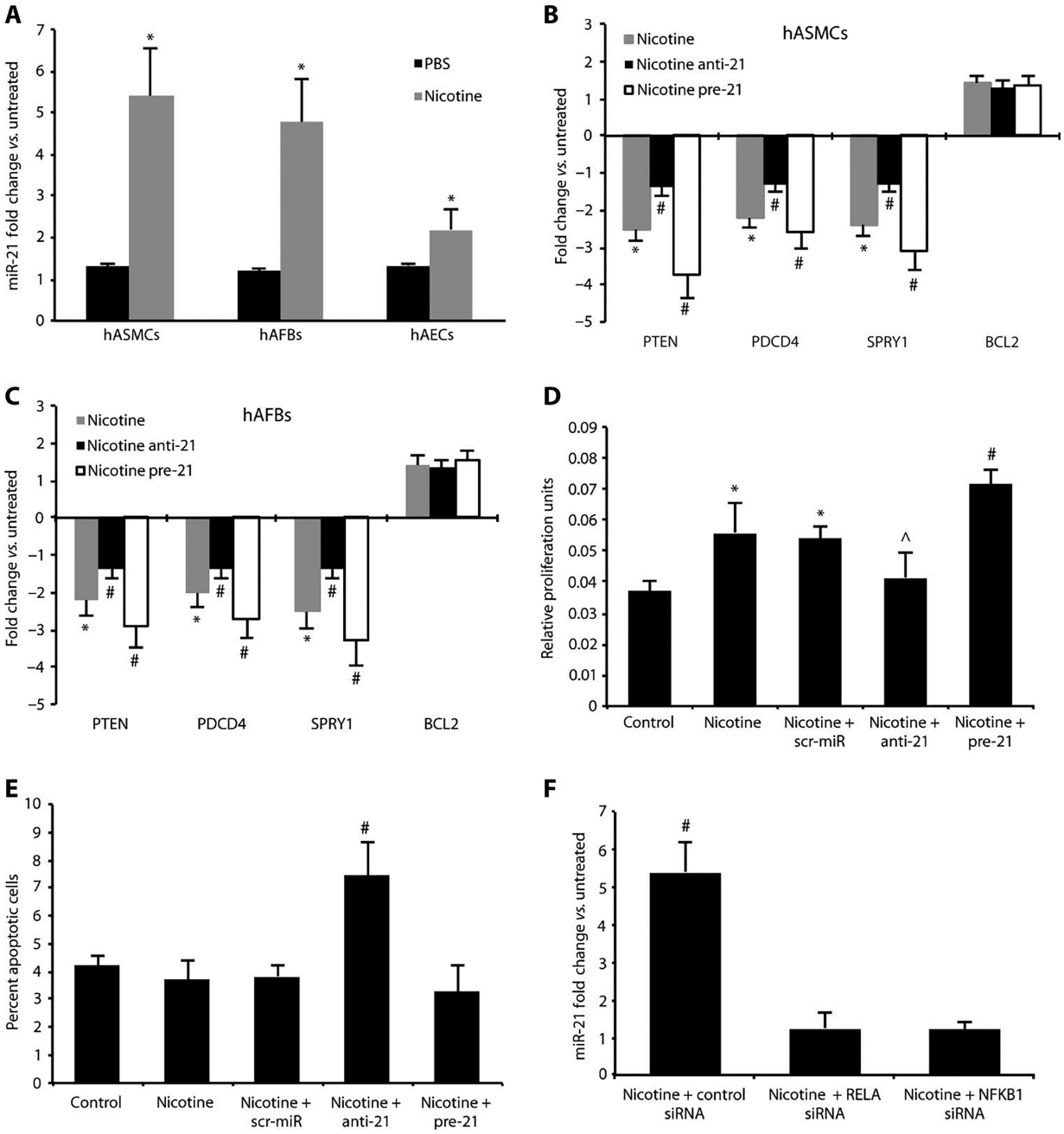

Fig. 2.

Effects of nicotine and miR-21 modulation in vitro. (**A**) miR-21 expression in nicotine (10 nM)– and PBS-treated (control) cultured hASMCs, hAFBs, and hAECs. (**B** and **C**) Expression of miR-21 target genes in nicotine-treated hASMCs (B) or hAFBs (C) transfected with miRNAs that block (anti-21) or boost (pre-21) miR-21 expression. (**D**) Proliferation of hASMCs after nicotine and pre-21 treatment was measured using the MTT assay. (**E**) Apoptosis of hASMCs after anti-21 treatment was measured by detecting the percent of annexin V–positive cells. (**F**) Knockdown of NF-κB subunits (RELA and NFKB1) with siRNA in nicotine-treated hASMCs. Data are means ± SEM. **P* < 0.05 versus

untreated control; #$P < 0.05$ for anti-21 andpre-21 (+nicotine) versus scr-miR and saline control (or nicotine + control siRNA versus nicotine + RELA/NFKB1 siRNA and versus untreated); ^$P < 0.05$ versus pre-21, scr-miR, and nicotine alone. Level of significance was determined using one-way ANOVA with Bonferroni's post test.

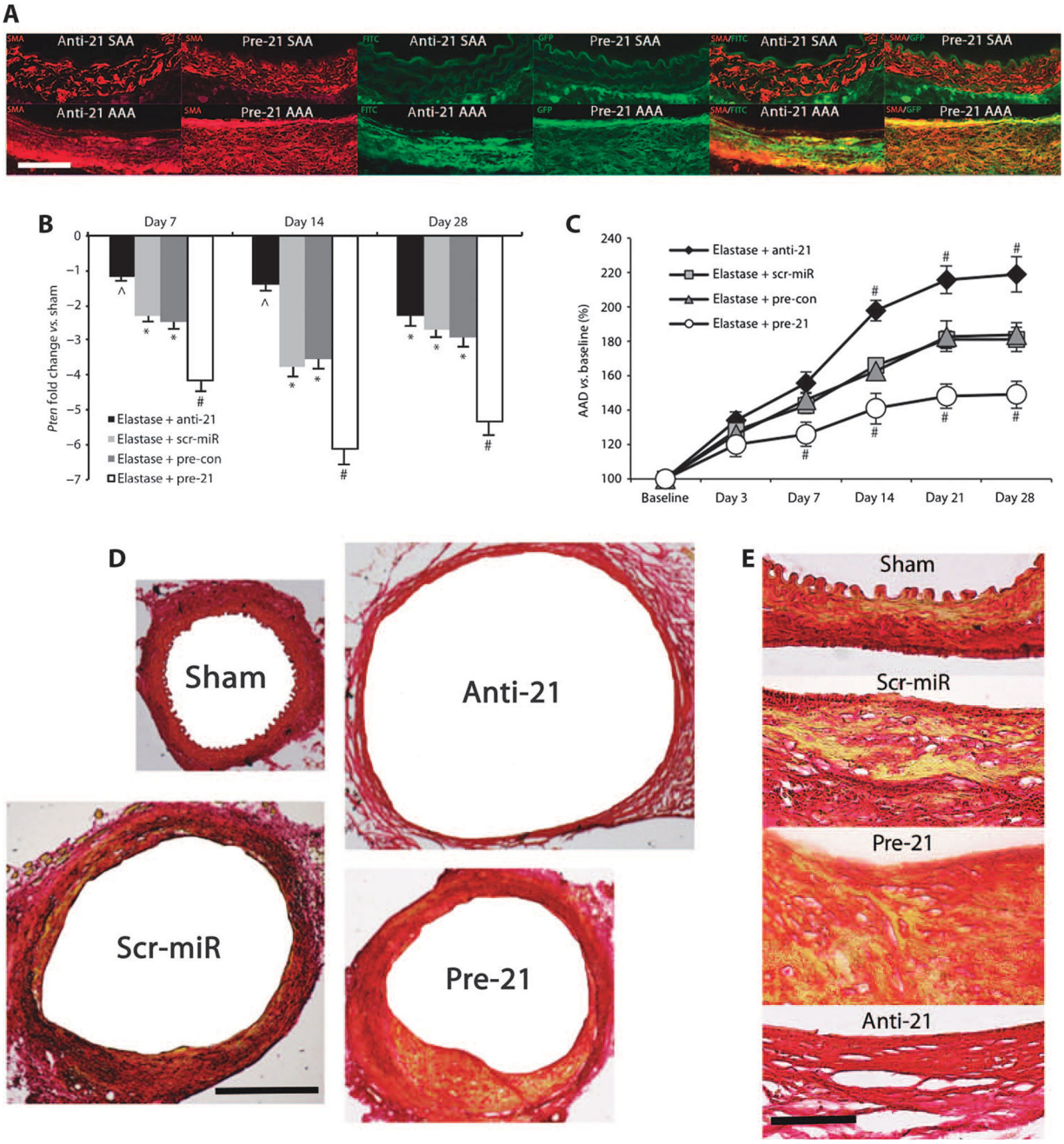

Fig. 3.

Effects of anti-21 and pre-21 in vivo. (**A**) Double immunofluorescence images for SMA (red) and GFP/FITC label (green) in the non-aneurysmal part of the suprarenal abdominal aorta (SAA) and in the infrarenal site of injury (AAA) in AAAs from mice treated with anti-21 or pre-21 (as single-color and merged images; labels on luminal side; scale bar, 50 μm). (**B**) *Pten* expression in elastase-induced AAA after treatment with anti-21, pre-21, scr-miR, or empty vector control (pre-con) compared to saline-infused mice (sham). (**C**) AAD (versus baseline as a percentage) in anti-21– and pre-21–transduced mice compared to scr-miR and empty vector control (pre-con) in the elastase infusion model of AAA. (**D** and **E**)

Representative low-power [(D) scale bar, 400 μm] and high-power [(E) scale bar, 50 μm] images of aortic cross sections stained with Picrosirius Red to illustrate differences in vascular wall structure (yellow/orange, muscle; red, collagen) in the aortic wall in anti-21– and pre-21–transduced mice compared to saline-infused controls (sham) and scr-miR in the elastase infusion model of AAA 28 days after induction. Scale bar, 50 μm. $n = 4$ to 8 mice for each time point and group. Data are means ± SEM. $*P < 0.05$ versus sham; $\#P < 0.05$ versus scr-miR/pre-con and sham; $\wedge P < 0.05$ versus sham and pre-21. Level of significance was determined using one-way ANOVA with Bonferroni's post test. Sequential measurements (AADs at consecutive time points) were analyzed by one-way repeated-measures ANOVA.

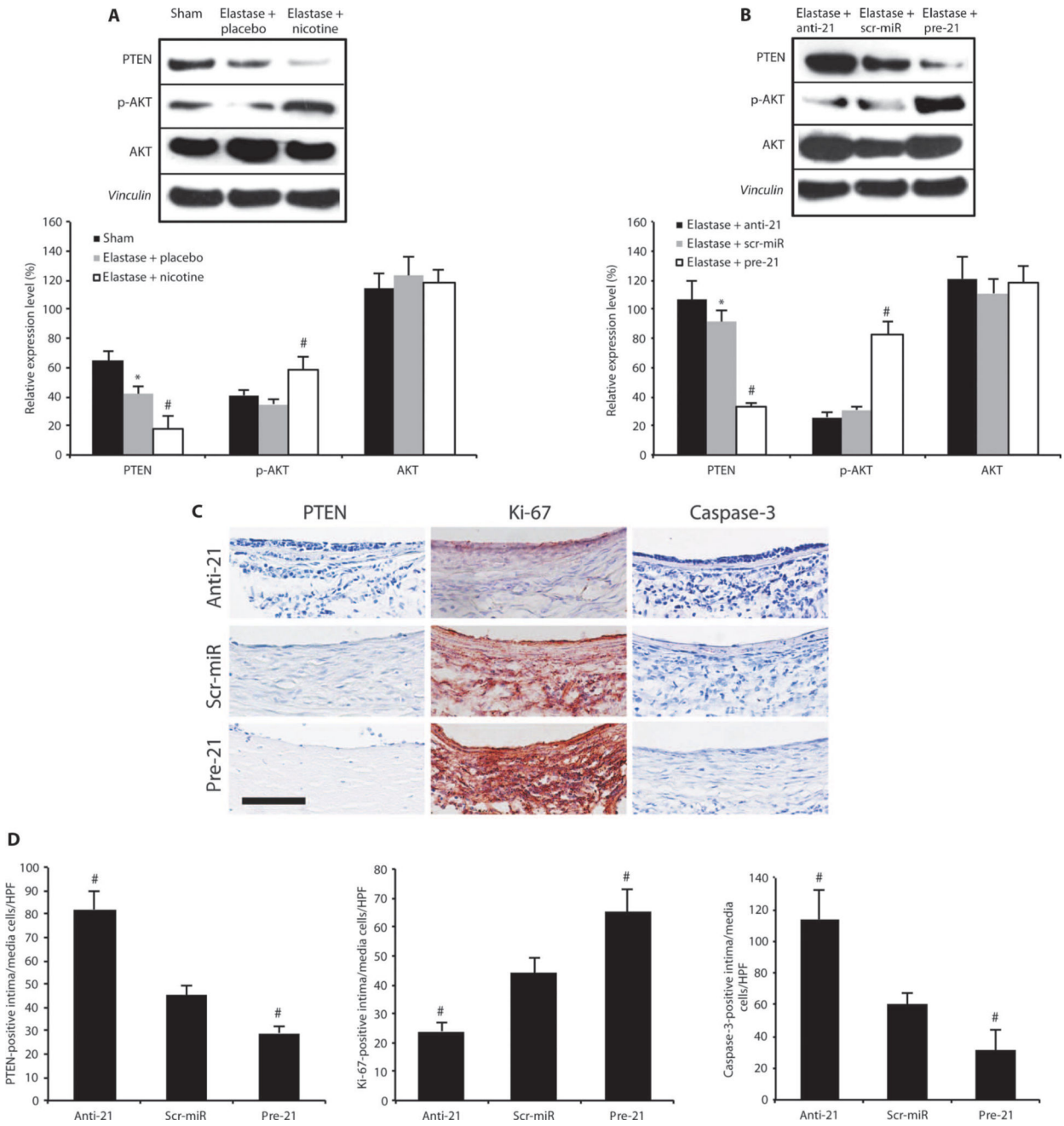

Fig. 4.

PTEN and p-AKT regulate proliferation and apoptosis in AAAs. (**A**) Representative immunoblots and expression levels for PTEN, p-AKT, and AKT relative to vinculin (loading control) in AAAs in elastase-infused mice (14 days after AAA induction) supplemented with either placebo or nicotine compared to saline-infused controls (sham; $n = 3$ to 4 mice per group). (**B**) Representative immunoblots and expression levels for PTEN, p-AKT, and AKT relative to vinculin (loading control) in AAAs in elastase-infusedmice (14 days after induction) transduced with anti-21 or pre-21 compared with scr-miR ($n = 3$ to 4 mice per group). (C**)** Representative immunohistochemical images demonstrating effects of treatment

with anti-21, pre-21, or scr-miR 14 days after AAA induction with elastase on PTEN expression (blue), cell proliferation (red positive for Ki-67), and apoptosis (purple-blue positive for caspase-3). Scale bar, 50 μm. (**D**) Quantification of PTEN-positive, Ki-67–positive, and caspase-3–positive cells in the intimal and medial region of AAAs. n=4 high-power fields (HPF) of 3 different aortas per group (12 total per group) 14 days after AAA induction. Data are means ± SEM. *P < 0.05 versus saline-infused controls (sham); #P < 0.05 versus scr-miR and versus sham (or versus elastase + placebo and versus sham). Level of significance was determined using one-way ANOVA with Bonferroni's post test.

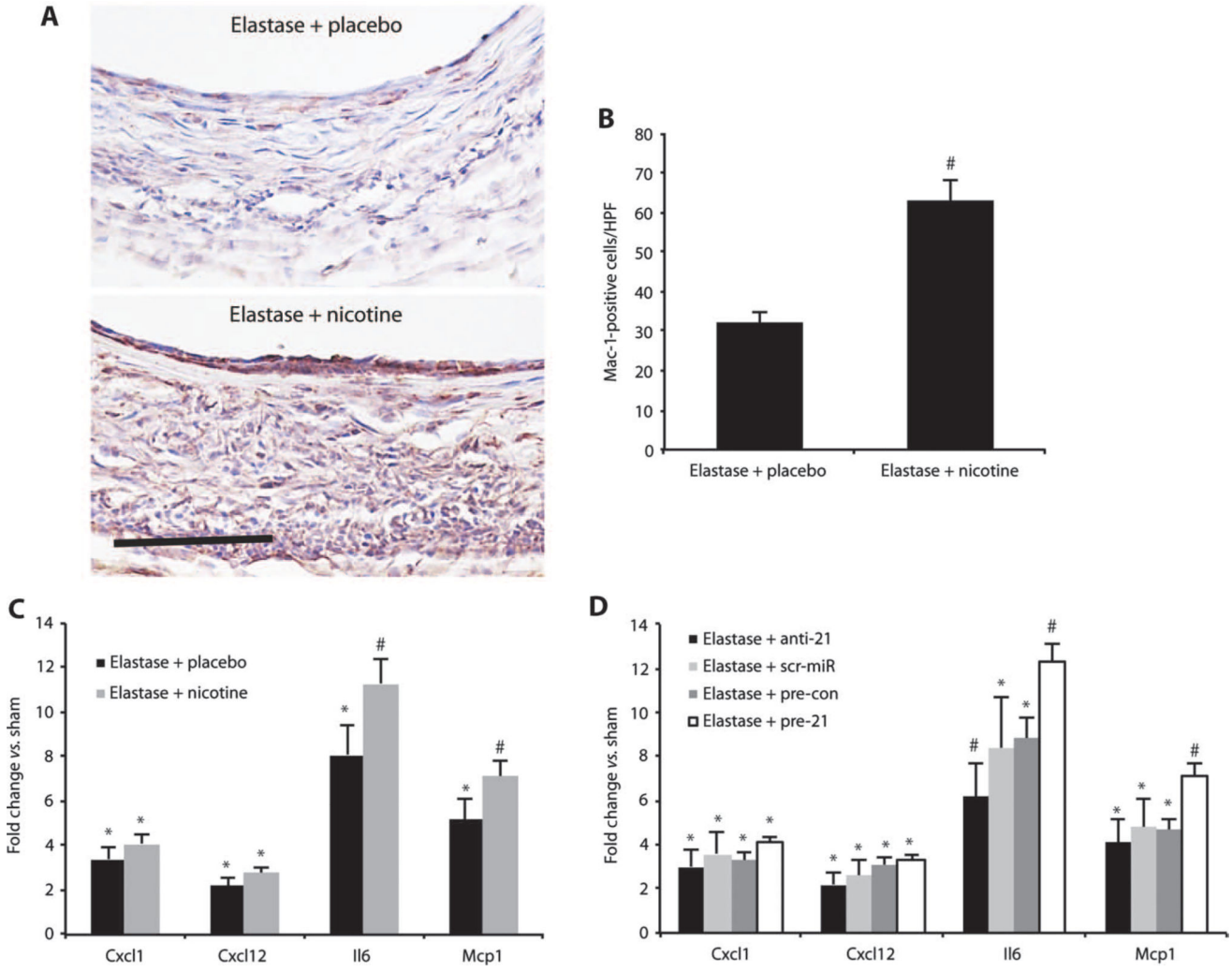

Fig. 5.

Nicotine triggers inflammation. (**A**) Mac-1–positive cells (red) are increased in mice supplemented with nicotine compared to placebo in the elastase-induced mouse model of AAAs. Scale bar, 50 μm. (**B**) Mac-1–positive cells from $n = 4$ high-power fields (HPF) from 3 different mice per group (12 total per group). (**C**) Gene expression of *Cxcl1, Cxcl12, Il6*, and *Mcp1* in mice infused with elastase and supplemented with either nicotine or placebo compared with saline-infused control mice (sham). (**D**) Gene expression of *Cxcl1, Cxcl12, Il6*, and *Mcp1* in mice transduced with anti-21 or pre-21, scr-miR, or empty vector control (pre-con) compared to sham 14 days after induction of AAA by elastase infusion. $n = 3$ to 7 per treatment group. Data are means ± SEM. *$P < 0.05$ versus sham; #$P < 0.05$ versus scr-miR, empty vector control (pre-con), and sham (or versus elastase + placebo and versus sham). Level of significance was determined using one-way ANOVA with Bonferroni's post test, or Student's *t* test for parametric measures (B).

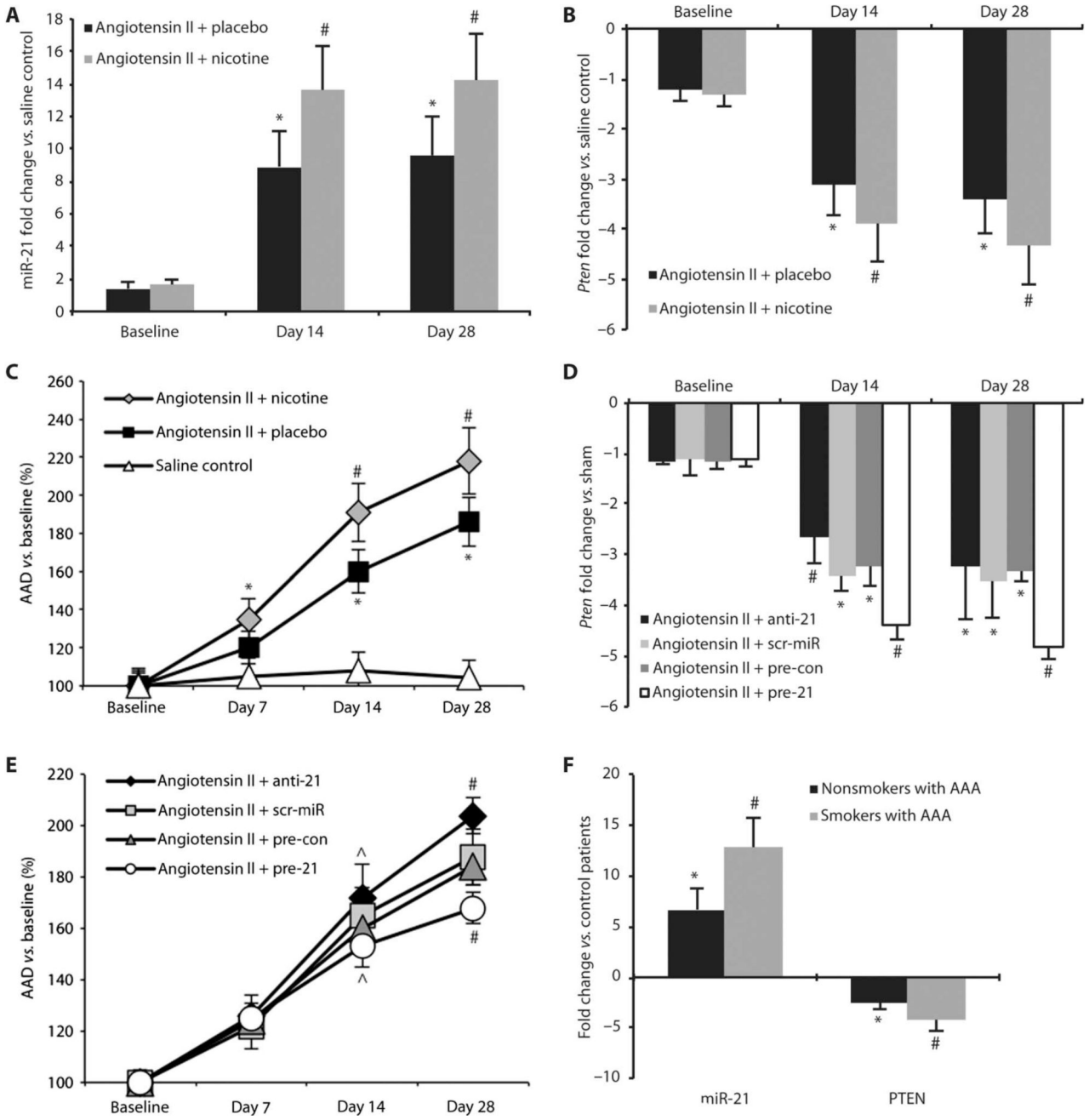

Fig. 6.

miR-21 and PTEN expression in mouse and human AAAs. (**A**) miR-21 expression in nicotine-treated and placebo-implanted mice infused with angiotensin II to induce AAAs compared to saline-infused control mice. (**B**) *Pten* expression in nicotine-treated and placebo-implanted mice infused with angiotensin II to induce AAAs compared to saline-infused control mice. (**C**) Expansion (as a percentage of baseline) of the AAD for nicotine-treated ($n = 35$) and placebo-implanted mice ($n = 28$) infused with angiotensin II to induce AAAs compared to saline-infused control mice ($n = 18$). (**D**) *Pten* expression in anti-21– and pre-21–transduced mice, mice treated with scr-miR, or empty vector control (pre-con)

compared to saline-infused control mice in the angiotensin II model of AAA. (**E**) AAD (as a percentage of baseline) in anti-21– and pre-21–transduced mice, as well as mice treated with scr-miR or empty vector control (pre-con) in the angiotensin II model of AAA. (**F**) Up-regulation of miR-21 and down-regulation of PTEN in human AAA tissue ($n = 5$ nonsmokers, $n = 8$ smokers) undergoing surgical repair compared to aortic samples from control patients without AAA ($n = 5$). Data are means ± SEM. *$P < 0.05$ versus saline controls (or control patients); #$P < 0.05$ versus placebo with angiotensin II and saline controls, scr-miR or pre-con, or nonsmokers and control patients; ^$P < 0.05$ versus angiotensin II with anti-21 or pre-21. Level of significance was determined using one-way ANOVA with Bonferroni's post test. Sequential measurements (AADs at consecutive time points) were analyzed by one-way repeated-measures ANOVA.